1 **The ecological relevance of fast-cycling mineral-associated organic matter – a dynamic pool**

2 **of 'persistent' soil carbon and nitrogen**

3

4 **Authors:** Andrea Jilling[1], A. Stuart Grandy[2], Amanda B. Daly[2], Rachel Hestrin[3], Angela

5 Possinger[4], Rose Abramoff[5], Madison Annis[1], Anna M. Cates[6], Katherine Dynarski[7], Katerina

6 Georgiou[8], Katherine Heckman[9], Marco Keiluweit[10], Ashley K. Lang[11], Richard P. Phillips[12],

7 Katherine Rocci[13], Itamar A. Shabtai[14], Noah W. Sokol[15], and Em Whalen[16]

8

9 [1]Department of Environmental Health Sciences, University of South Carolina, Columbia, SC

10 [2] Center of Soil Biogeochemistry and Microbial Ecology, Department of Natural Resources and the

11 Environment, University of New Hampshire, Durham NH 03824

12 [3]Stockbridge School of Agriculture, University of Massachusetts Amherst, Amherst, MA 01003

13 [4]School of Plant and Environmental Sciences, Virginia Tech, Blacksburg, VA 24061

14 [5]School of Forest Resources, University of Maine, Orono, ME 04469

15 [6]Department of Soil, Water, and Climate, University of Minnesota, St. Paul, MN 55108.

16 [7]USDA-Natural Resources Conservation Service, Soil and Plant Science Division, National Soil Survey

17 Center, Lincoln, NE 68508.

18 [8]Department of Biological & Ecological Engineering, Oregon State University, Corvallis, OR

19 [9]Northern Research Station, USDA Forest Service, Houghton, MI 49931

20 [10] Institute of Earth Surface Dynamics, University of Lausanne, Lausanne 1015 CH, Switzerland

21 [11] USDA Forest Service Northern Research Station, St. Paul, MN 55108

22 [12] Department of Biology, Indiana University, Bloomington, IN 47405

23 [13]Institute of Arctic and Alpine Research, University of Colorado, Boulder, CO, 80309; Institute for Global

24 Change Biology, University of Michigan, Ann Arbor, MI, 48109

25 [14]Department of Environmental Science and Forestry, Connecticut Agricultural Experiment Station, New

26 Haven, CT 06511

27 [15]Physical and Life Sciences Directorate, Lawrence Livermore National Laboratory, Livermore, CA, USA

28 94550

29 [16]Critical Ecology Lab, Oakland, CA, 94610

30

31

32

33 **Figures:** 1

34 **Tables:** 2

35

36 **Correspondence:** Andrea Jilling (ajilling@mailbox.sc.edu)

37

38

39

Abstract

Longstanding theories and models classify mineral-associated organic matter (MAOM) as the large (~60%) but slow-cycling and persistent portion of the soil organic matter (SOM) pool. Strong physico-chemical interactions and diffusion limitations restrict the turnover of MAOM, allowing carbon and nitrogen bound therein to persist in soil for as long as centuries to millennia. However, MAOM is a chemically and functionally diverse pool with a substantial portion cycling at relatively fast (i.e., minutes to years) timescales. Despite a growing body of evidence for the heterogenous and multi-pool nature of MAOM, we lack consensus on how to conceptualize and directly quantify fast-cycling MAOM and its ecological significance. We demonstrate the dynamic qualities of fast-cycling MAOM vary based on 1) the chemistry of the mineral particles and organic matter, 2) the complex set of interactions between OM and the mineral matrix, and 3) the presence and strength of destabilizing forces that lead to decomposition or loss of MAOM (i.e., plant-microbe interactions, land use change, agricultural intensification, and climate change). Finally, we discuss potential implications and research opportunities for how we measure, manage, and model the dynamic subfraction of this otherwise persistent pool of SOM.

1. Introduction

Soil organic matter (SOM) plays a central role in terrestrial ecosystem functioning, providing nitrogen (N) and other nutrients to plants, and holding the largest pool of organic carbon (C) on

64 land. A portion of the SOM pool cycles slowly – with turnover time ranging from decades to

65 millennia. Our understanding of SOM persistence has evolved from an emphasis on chemical

66 complexity and "recalcitrance" towards a growing appreciation for the interactions between

67 relatively simple plant and microbial inputs and reactive mineral surfaces as key controls on

68 SOM persistence[1]. As such, there is considerable focus on characterizing and measuring the

69 mineral-associated organic matter (MAOM; see Box 1) pool, the fraction of SOM which holds

70 the majority of organic C and N in the terrestrial biosphere (~60% of C and 75% of N)[2]. Strong

71 physico-chemical interactions and diffusion limitations restrict the turnover of some MAOM,

72 allowing C within this pool to persist for centuries to millennia [3].

73

Box 1: MAOM definitions and characteristics

Mineral-associated organic matter (MAOM) is the term used to describe both a conceptually-defined and methodologically-defined fraction of soil organic matter (SOM). Conceptually, MAOM is defined as a fraction of SOM where OM exists in some degree of association with soil minerals, such as via sorption, co-precipitation, encapsulation in fine, micro-aggregates sensu Lehmann et al.[4], or via organo-organo interactions. MAOM is typically defined in contrast to sand-sized and less protected material known as particulate organic matter (POM). The methodological definition of MAOM is material collected from soil (generally, operationally defined as < 2mm) with aggregates dispersed by physical (i.e., glass beads), chemical (i.e., dispersing agents like sodium hexametaphosphate), or energetic (i.e., sonication) methods and then collected as the fraction passing through a 50-63 µm sieve (i.e., the silt- and clay-sized particles) and/or with a density greater than 1.6-1.85 g cm^{-3} (i.e., the heavy fraction). Operational definitions of MAOM (e.g., as defined by a small particle size or

---

heavier density) are not always fully aligned with conceptual definitions. Size separations can also capture partially decomposed plant and fungal components not associated with minerals in the fine fraction, and density separations may capture SOM associated with sand in the heavy fraction. Recent work has found that combining size and density separation methods can minimize these artifacts[5].

74

75   Particulate organic matter (POM) is considered a more bioavailable and faster cycling

76   pool of soil C and N, relative to MAOM. POM is dominated by larger fragments of plant and

77   microbial residues, which are at early stages of decomposition. The POM pool responds rapidly

78   to changes in tillage or plant inputs and often correlates strongly with whole soil measures of

79   decomposition[6], contributing to the view of POM as an SOM pool that is particularly sensitive to

80   disturbances and physically accessible to decomposers. However, the decomposition of POM, in

81   addition to litter decomposition, is also needed to build MAOM[7]. The leaching and

82   depolymerization of POM and litter releases OM compounds into solution, which can then

83   adsorb to a reactive mineral surface before or after cycling through microbial biomass[8–10]. While

84   microaggregates provide further protection to MAOM[11], aggregate turnover and disturbance

85   promote MAOM formation as well[12]. MAOM formation is also more efficient within the

86   rhizosphere relative to the bulk soil, which suggests MAOM forms under highly dynamic

87   conditions[13]. MAOM formation is fast: transfer of ^{15}N or ^{13}C-labeled plant residues into MAOM

88   fractions can occur within days to months[14–17].

89   The abundance of fine mineral particles and mineral specific surface area are strong

90   predictors of soil C storage[18,19]. As such, MAOM is often examined for its capacity to store and

91   sequester C and nutrients, with less attention on the heterogeneity underlying the MAOM

92 fraction and its implications for potential destabilization following disturbance (for exceptions,

93 see Bailey et al. and Dynarski et al.)[20,21]. Although the majority of MAOM is likely persistent

94 and long-lived, there is increasing evidence for a dynamic, fast-cycling MAOM pool.

95   Given the vast quantity of C and N stored in MAOM, the presence of even a small active

96 MAOM pool can substantially influence ecosystem processes. For example, a hypothetical and

97 very conservative annual MAOM turnover rate of 1% in a grassland with 3,000 kg MAOM N ha$^-$

98 ^{1} in the top 10 cm of soil[22] would supply 30 kg N ha^{-1} per year, which is approximately a third of

99 the N uptake by grassland species[23]. The fast-cycling MAOM pool may function as a distinct

100 SOM pool with essential roles in ecosystems, including retaining nutrients prone to loss and

101 supplying nutrients to plants and microbes. At the same time, this fast-cycling MAOM pool may

102 become a larger source of greenhouse gas emissions over time, especially under accelerated land

103 use and climate change, as we discuss below.

104   The idea of a fast-cycling MAOM pool is not new (e.g., Kleber et al. and Torn et al.)[24,25],

105 but the concept is rarely acknowledged in research and policies related to the management of

106 MAOM (e.g., natural climate solutions-oriented work) or in Earth system models. In this review,

107 we seek to clarify the existence and ecological importance of fast-cycling MAOM with a

108 targeted summary of research on this crucial SOM pool. Others have synthesized relevant

109 geochemical mechanisms of mineral-organic interactions[26] and the land use and climate change

110 implications of POM versus MAOM[27] but have not focused explicitly on the fast-cycling

111 MAOM pool. Here, we synthesize recent studies that confirm the existence of a fast-cycling

112 MAOM pool across various ecosystem types and provide insight into its size, stability and

113 mechanisms of turnover. We describe its key role in ecosystem functions such as nutrient

114   provisioning, soil C cycling, and plant-microbe interactions, and suggest implications for how

115   we measure, manage, and model this dynamic subfraction of MAOM.

116

117   ***2. MAOM is chemically heterogeneous***

118

119   MAOM is a large and heterogenous pool of SOM, containing mineral particles and

120   organic molecules that vary widely in age, size, and reactivity. Variations in MAOM binding

121   mechanisms and chemical characteristics determine how this pool of OM cycles through

122   terrestrial ecosystems, by influencing its availability to microbes, turnover rate and potential to

123   serve as a plant nutrient source. At the scale of mineral surface-OM associations, the behavior of

124   MAOM and the chemical bonds therein will depend largely on characteristics of the interacting

125   organic compounds, mineral particles and soil solution[26,28–31](Figure 1). Minerals can have

126   permanent and/or variable charges of varying strength, distribution, and density and such

127   differences will impact the type and number of binding sites, adsorption-desorption behavior,

128   and hence, the bioavailability of associated molecules[32,33]. For example, minerals with a

129   relatively high point-of-zero-charge that are positively charged under neutral and acidic

130   conditions, such as goethite, may be able to bind SOM more strongly via ligand exchange

131   reactions compared to negatively charged clay minerals that bind to OM via cation bridging[34].

132   Mineral types that bind compounds more weakly may harbor more vulnerable and accessible

133   forms of MAOM.

134   Characteristics of organic substrates expected to influence the mechanism and strength of

135   association include molecular size, hydrophobicity, acidity, and abundance of carboxylic,

136   phenolic and aromatic constituents, which interact with mineral surface chemistry to influence

137 the mechanism and reversibility of organo-mineral associations[35–37]. For example, stronger

138 covalent bonds tend to form between organic substrates enriched in aromatic acid and phenolic

139 groups and mineral fractions with a high abundance of reactive Fe and Al (oxy)hydroxide

140 phases, especially under acidic soil solution conditions [36,38]. Stoichiometry (e.g., the C:N ratio) of

141 organic matter will also influence its potential for adsorption or desorption[39]. Empirical work and

142 direct imaging of organo-mineral interfaces at sub-micron scales indicate that N-rich organic

143 compounds (e.g., N-containing groups in proteins) bind preferentially to mineral surfaces[40–45],

144 and it is often suggested that MAOM-N is more stable than MAOM-C as a result.

145   The stability and turnover dynamics of MAOM are also shaped by its fine-scale spatial

146 and compositional heterogeneity[4,43,46–49]. Several lines of evidence support the existence of

147 spatially or chemically distinct portions of MAOM that are more vulnerable to mineralization.

148 Kleber et al. proposed a model suggesting that OM binds to mineral surfaces in a zonal

149 structure[24]. In this multi-layer model, the outermost zone is referred to as the "kinetic zone" and

150 hosts organic molecules that are weakly bound via van der Waals forces, hydrogen bonding, and

151 cation bridging interactions. Secondary interactions among organic molecules (i.e., organo-

152 organic interactions[43]) are consequently an important mechanism within this kinetic zone, and

153 provide a mechanism for loading of new organic substrates to pre-existing MAOM [31,49]. In the

154 zonal model, the more weakly-associated kinetic material is hypothesized to exchange readily

155 with the soil solution. Similarly, Kaiser and Guggenberger argued that the potential

156 bioavailability of MAOM depends on the degree of OM loading on mineral surfaces[50,51]. As

157 more organic molecules occupy binding sites, a proportion of MAOM may become more

158 susceptible to degradation due to fewer functional groups being involved in sorption. Further, the

159 enrichment of N-rich OM at the mineral surface is consistent with a zonal model driven by

160   preferential retention of N-containing functional groups (e.g., through hydrogen bonding, cation

161   bridges, or ligand exchange)[28]. However, in batch adsorption experiments using dissolved

162   organic matter (DOM) and goethite, Coward et al. found that N-containing compounds were the

163   last to adsorb, populating the "kinetic" zone, which is hypothesized to constitute the most

164   dynamic, exchangeable fraction[52]. Variations in mineral-organic interactions, including those

165   regulated by variation in chemical bonds, organic matter composition and fine-scale spatial

166   heterogeneity, warrants deeper engagement with the idea of MAOM containing a fast cycling

167   and bioavailable subfraction.

168

169   *3. MAOM contains young and mineralizable compounds*

170

171   MAOM is generally characterized as old and slow-cycling due to a consistent increase in SOC

172   mean residence time (aka 'mean system age')[53] with decreasing particle size. Radiocarbon

173   analyses demonstrate that silt- and clay-associated OM has a longer estimated turnover time than

174   sand-associated OM[54]. However, a small but fast-cycling portion of MAOM (i.e., days to years)

175   may be obscured in these estimates by much slower-cycling compounds (i.e., centuries to

176   millennia) that substantially shift the mean estimate of residence time in these observational

177   studies[55,56]. Radiocarbon tracer studies can more accurately track the rate of incorporation of new

178   inputs to MAOM, though they are rarely employed. However, one site in an oak forest with

179   accidental radiocarbon release found that up to 37% of MAOM is replaced on an annual basis,

180   implying a mean residence time of four years[57]. In the same soils, the steady-state mean

181   residence time estimated from natural abundance radiocarbon measurements was 108 years,

182   which suggests that natural abundance-based averages may not be a reliable measure of typical

183   MAOM residence times in topsoil[57].

184   Recent work suggests that a primary driver of skewness in radiocarbon-based SOM and

185   MAOM age data may be organic fossil C in sedimentary soil parent materials, including

186   kerogen, lignite, and coal, which could contribute substantially to MAOM C pools. The

187   presence of fossil C may skew radiocarbon ages in MAOM and other SOM fractions[58–60]. The

188   use of ramped thermal analysis has proved an effective means of illustrating how the average

189   radiocarbon value of a MAOM fraction may obscure the strongly contrasting "ages" of its

190   constituent compounds, which may range from post-bomb (modern) to nearly radiocarbon dead

191   (~60,000 years old or older)[61]. Thus, the reliance on radiocarbon dating alone to infer the mean

192   age or persistence of MAOM may lead to spurious conclusions regarding MAOM durability in

193   the context of climate change and its potential to store new C additions over long timescales.

194   Mineral surfaces provide MAOM with some protection from decomposition, but they are

195   also host to active microbial communities. Mineral surfaces support high microbial biomass and

196   accelerated rates of microbial turnover and enzyme production[62–64]. The abundance of low-

197   molecular weight and low C:N compounds support a high mineralization potential within

198   MAOM [65]. The intrinsic bioavailability of MAOM is illustrated by several incubation-based

199   experiments. In a study of 156 diverse soils from across the United States, Yu et al. demonstrated

200   that both MAOM and POM are strong predictors of whole soil C decomposition dynamics[66].

201   They suggest that the large pool size of MAOM may compensate for its lower decomposition

202   rates in some soils creating similar overall contributions to CO_2 flux as POM. When SOM

203   fractions are incubated under ideal temperature and moisture conditions, MAOM can even

204   exhibit higher N and C mineralization potential compared to POM or light fractions [67–72]. This

205   was recently observed for soils collected from forest, grassland, and cropland land uses [73].

206   Two main methodological approaches provide direct estimates of the potentially

207   bioavailable and fast-cycling portion of the MAOM pool: (1) isotope tracer mineralization

208   experiments and (2) batch adsorption-desorption experiments. Isotope tracer mineralization

209   experiments, which trace the decomposition of clay-bound organic compounds over the course

210   of days or weeks-long incubations, demonstrate an intrinsic capacity for MAOM to supply C and

211   N (Table 1). Over half of adsorbed organic compounds in such experiments were bioavailable

212   and mineralizable, with the magnitude of decomposition often mediated by mineral type (Table

213   1).

214   Batch adsorption-desorption studies highlight how rapidly compounds may desorb from

215   mineral surfaces (Table 2). Such experiments quantify the equilibrium partitioning of a sorbate

216   between solid and solution phases, in a liquid suspension over 24-48 hours[74] and using a wide

217   range in soil:solution ratios (1:4 to 1:10,000). Results demonstrate the rapid and largely

218   irreversible adsorption of organic compounds. However, approximately half of adsorbed OC can

219   be removed with water within a few hours, which highlights the high potential bioavailability of

220   MAOM. Reported rates of desorption vary widely due to the variety of experimental conditions

221   including mineral type, desorption agents, background electrolytes, and pH. Likewise, the short

222   duration, highly disturbed, and often artificial context limit our ability to interpret and translate

223   results to natural soil systems. Nonetheless, laboratory experiments tracing the desorption and

224   mineralization of OC from clays as in Tables 1 and 2 highlight the potential for microbes and

225   plant roots to access and decompose MAOM. As will be discussed below, there are certain

226   ecological contexts and processes that may allow for this mineralization potential to be realized

227   at the ecosystem scale.

228

229   *4. Ecological Drivers of MAOM Destabilization*

230

231   While there has been much emphasis on the controls of SOM formation and persistence, a

232   growing body of research has focused on the drivers of SOM destabilization[20]. Forces of

233   destabilization have been categorized into those that disrupt soil physical structure (such as soil

234   aggregates), those that disrupt mineral-organic associations, and those that enhance C

235   metabolism[20]. Below, we focus on three proximal drivers of MAOM destabilization: plant-

236   microbial interactions, climate change, and agricultural intensification. The transfer of OM from

237   mineral-associated to more bioavailable pools will depend on the presence and strength of

238   particular environmental conditions that favor MAOM destabilization.

239

240   *4.1. Plant-microbial forces*

241

242   Rhizosphere environments provide conditions that can facilitate the destabilization and turnover

243   of MAOM. MAOM in the rhizosphere is more likely to be released from mineral surfaces than

244   MAOM in bulk soil due to a higher concentration of plant and microbial exudates in the soil near

245   active roots[75,76]. These exudates may stimulate specific extracellular enzymes or more generally

246   stimulate decomposition (i.e. glucose, organic acids). Additionally, plant and microbial exudates

247   can form associations with soil minerals directly, contributing to the MAOM pool[77]. In fact, root-

248   derived organic matter, particularly root exudates, is suggested to be a dominant source of

249 mineral-associated C and N[13,78–81]. As a result, rhizosphere MAOM acts as both a source and

250 sink for organic compounds and is likely more dynamic compared to MAOM in the bulk soil.

251 MAOM may be particularly vulnerable to destabilization by plant exudates in ecosystems

252 with rapidly growing vegetation and high demand for soil nutrients. These conditions are

253 common in early successional forests, agricultural systems, and ecosystems recovering from

254 disturbance or responding to global change[82–84]. Some evidence for these patterns comes from

255 analyses of MAOM radiocarbon content where in the eastern U.S., MAOM turns over more

256 quickly in ecosystems with higher root mass[85]. This suggests that ecosystems with high plant

257 nutrient demand may have a higher proportion of fast-cycling MAOM compared to other

258 ecosystems, particularly in the rhizosphere.

259 The rhizosphere is also characterized by the presence and enrichment of mineral-

260 weathering soil bacteria. Rhizosphere activity can accelerate the formation of metal oxides[86] or

261 facilitate rock weathering and clay transformation processes[87–89]. Phosphate-dissolving bacteria

262 have been reported in the rhizosphere of agricultural soils [90] and around the roots of mangrove

263 trees [91]. Similarly, the dissolution of clay particles was highest in rhizosphere of Norway spruce

264 and oak compared to bulk soil [92]. Although mineral weathering is generally seen as a slow

265 pedogenic process, it can occur over short time scales, especially in the microbially active zone

266 around roots. Processes occurring at the root-soil interface can significantly accelerate

267 pedogenesis such that mineral dissolution or alteration can occur within 20 years[92,93] or even

268 within a growing season[94]. It is unclear how these localized, accelerated alterations to clay

269 particles in the rhizosphere alter the formation and cycling of MAOM specifically.

270 Mycorrhizal fungi, which receive energy-rich carbon compounds from plant hosts, are

271 equipped to destabilize and mobilize MAOM. The capacity for ectomycorrhizal fungi (ECM) to

272   liberate MAOM was recently reviewed by Tunlid et al[95]. Many ECM fungi secrete low

273   molecular weight compounds like oxalic acid that can disrupt mineral-organic associations [96],

274   dissolve minerals [97], release nutrients [95] and facilitate the direct assimilation of N from MAOM[98].

275   Some ECM species also mediate the reductive dissolution of iron-bearing minerals and the

276   subsequent generation of reactive oxygen species[99]. MAOM was shown to be more sensitive to

277   hydroxyl radicals than POM, which was attributed to the enrichment in MAOM of low

278   molecular weight compounds with lower activation energies[100]. Thus, ECM-facilitated

279   dissolution of minerals may accelerate the decomposition of MAOM. Arbuscular mycorrhizal

280   fungi (AMF) also generate many of the same compounds with known weathering capacities[101,102]

281   but may have limited capacity to mobilize MAOM. AMF rely on bacterial-mediated

282   decomposition to access inorganic N[103] as their enzymes are not as effective at mining nutrients

283   directly from SOM. AMF-generated organic acids were shown to mobilize phosphorus bound to

284   iron oxides[104], but this area of research remains highly understudied. Overall, evidence suggests

285   that the activities of roots, mycorrhizal and free-living microbes contribute substantially to

286   MAOM mobilization, likely making the rhizosphere a hotspot for dynamic and fast-cycling

287   MAOM.

288

289   *4.2. Climate-related forces*

290

291   Climate is a major driver of plant growth, microbial activity, and abiotic properties of soils.

292   Therefore, it is also likely to alter the formation and destabilization of MAOM, with direct

293   implications for the fast-cycling MAOM pool. Shifts in climate may disrupt and alter MAOM

294   formation and destabilization processes, potentially limiting MAOM accrual and/or accelerating

295   the loss of MAOM. Multiple studies report how changes in precipitation, temperature, and

296   atmospheric CO_2 may destabilize MAOM across varied ecosystems.

297   Given projected shifts in climate toward intensification of hydrologic cycles, it is

298   important to understand how shifting moisture regimes may alter fast-cycling MAOM. In arid

299   systems where moisture limitation is a physiological control on microbial mineralization,

300   changing precipitation patterns (and increased DOC fluxes to subsoil) may facilitate MAOM

301   losses[85]. Moisture availability indices (e.g., MAP/PET) and correlated moisture-driven

302   mineralogy gradients (e.g., reactive metal vs. base cation-dominated mineralogy) have therefore

303   been applied as organizing concepts to predict differences in MAOM formation mechanisms[105–

304   108] and susceptibility to destabilization under changing moisture availability across broad-scale

305   climatic regions[107].

306   In addition to the role of moisture regime at the ecosystem scale, MAOM destabilization

307   processes are influenced by moisture-driven changes in soil redox status at the pore scale. Most

308   notably, the reduction of iron-bearing minerals under saturated conditions can release mineral-

309   bound C into soluble forms, leading to potential net losses of C following a return to oxic

310   conditions[109–113]. However, saturation may also cause more dynamic sorption-desorption events

311   in soils less dominated by iron-bearing minerals[114]. In environments experiencing frequent wet-

312   dry cycles, shifting aerobic to anaerobic conditions has been shown to increase the

313   bioavailability of MAOM, possibly due to a loss of Fe-MAOM associations[43]. Wet-dry cycling

314   was also shown to enhance the decomposition of MAOM and its vulnerability to simulated

315   exudates[115]. This suggests that increases in moisture variability due to climate intensification

316   may promote a larger fast-cycling MAOM pool.

317   Temperature is an important control on SOM decomposition rates [116], but the sensitivity

318   of faster-cycling MAOM components to changing temperature is less well described. In general,

319   MAOM is expected to be less temperature-sensitive overall compared to POM [117,118]. However,

320   there have been few direct studies of the responses of different components of MAOM to

321   changes in temperature. Available evidence suggests larger and lighter components of MAOM

322   are more responsive to warming[119,120]. One possibility, which warrants further investigation, is

323   that larger and lighter portions of MAOM are held more loosely to mineral surfaces, making

324   them more susceptible to mineralization with increased microbial activity. In addition, Possinger

325   et al. found that OM protected by reactive metal associations was more vulnerable to warming

326   temperatures than OM protected by base cations, potentially due to the temperature sensitivity of

327   biological processes involved in overcoming stable organo-metal interaction mechanisms[107].

328   As the CO_2 fertilization effect promotes higher rates of photosynthesis, plants require

329   more nutrients from soil, particularly N[121]. As a result, rising atmospheric CO_2 concentrations

330   may indirectly promote MAOM desorption and turnover as a consequence of increasing plant

331   nutrient demand. In ecosystems without a large standing stock of bioavailable N, plants may rely

332   on MAOM as a source of limiting nutrients to fuel higher rates of productivity. This may occur

333   through greater root exudation[84], which could cause desorption of N-rich MAOM that would

334   subsequently be available for mineralization. However, rhizosphere-induced priming may also

335   act on the POM pool rather than the MAOM pool[122,123]. In support of minimal MAOM

336   responses, a meta-analysis of global change manipulations found no significant effect of elevated

337   CO_2 (eCO_2) on MAOM-C concentrations[118]. However, in studies conducted for more than five

338   years, MAOM-C concentrations tended to decrease with eCO_2[118]. This pattern suggests that the

339   effects of eCO_2 may not be immediately apparent, but could become more evident over time as

340 the diminishing soil nutrient pool prompts plants and microbes to begin mining resources from

341 MAOM.

342

343

344 *4.3. Land use change and agricultural management*

345

346 In general, land management that alters the input and microbial processing of OM will influence

347 MAOM cycling[124]. Agricultural management systems may shift disturbance regimes, external

348 inputs, and plant diversity, as well as the abiotic environment (e.g. temperature and moisture),

349 with both biotic and abiotic drivers influencing MAOM[115,125,126]. For example, the physical

350 disruption of tillage and changes in irrigation can disproportionately impact the MAOM

351 protected within macro-aggregates[127]. MAOM turnover also depends on the C:N ratio and

352 chemical composition of organic inputs. For example, a clover-rye mixed cover crop facilitated

353 transfer of POM-C to MAOM-C more than a rye or clover crop alone[128]. Manure additions have

354 been linked to faster MAOM turnover times than synthetic inputs[129], perhaps because inorganic

355 fertilizer applications may suppress the biological mechanisms that mobilize MAOM [130].

356   MAOM response to management depends on both MAOM formation and loss;

357 management that increases soil microbial activity can also enhance MAOM mineralization. The

358 balance between stabilization and destabilization processes is heavily context-dependent and

359 may result in either increases or decreases in MAOM[20]. For example, in a study on intensively

360 managed Mollisols, incorporating legume cover crops and adding manure did not result in

361 increased MAOM as hypothesized[131]. The researchers attributed this finding to nutrient mining

362 of MAOM by the maize crop, which offset potential gains in MAOM due to enhanced microbial

363 efficiency and biomass production. Similarly, long-term organic fertilization increased MAOM-

364 C turnover, but not accrual[129]. Organic cropping with manure on an Alfisol also did not increase

365 MAOM[132], but adding a legume cover crop did increase MAOM in an arid wheat cropping

366 systems on silt loam soils[133]. These studies highlight how measuring net changes overlooks

367 active-cycling MAOM, which may be a large flux in systems that experience high rates of both

368 MAOM loss and accrual. This fast-cycling MAOM may prove to be important in predicting N

369 available to crops, as N mineralization remains an important, and poorly predicted, element of

370 crop yield[130,134–136].

371   In some cases, management may not alter POM or MAOM quantity, but rather cause

372 shifts in the chemical composition of one or both fractions. For example, MAOM chemical

373 composition shifted in response to contrasting cover crop functional types[137] and organic

374 cropping systems with cover crops and manure[132], even though MAOM-C concentration was not

375 affected. Similarly, Teixeira et al. observed that with the shift from tropical savanna to pasture,

376 losses of savanna-derived MAOM-C were offset by gains from pasture-derived C[138]. These shifts

377 in MAOM chemical composition or quantity may correspond with faster-cycling MAOM, but it

378 is uncertain how to measure or manage plant access to this nutrient supply.

379

380

381 *5. Implications of the multi-pool and dynamic nature of MAOM*

382

383 The implications of a fast-cycling MAOM pool for both agricultural management and

384 representation within Earth system models have largely gone unexplored. Below, we discuss the

17

385 relevance of fast-cycling MAOM for these applications and highlight key research opportunities

386 to improve our understanding and measurement of this MAOM pool's importance.

387

388 *5.1. Managing fast-cycling MAOM in managed landscapes*

389

390 While some management practices may destabilize MAOM, there are other practices that may be

391 harnessed to promote fast-cycling MAOM for multiple benefits such as soil nutrient availability

392 and accrual of soil carbon. A recent review by Daly et al. outlined several key hypotheses about

393 the potential role of the fast-cycling MAOM pool that require further testing[130]. First, fast-

394 cycling MAOM can provide key nutrients for crops, particularly in low input systems that

395 promote plant investment in root production and mycorrhizal symbioses[130]. Furthermore, fast-

396 cycling MAOM may play a key role in the accumulation of more persistent SOC. Movement of

397 compounds into and out of the fast-cycling MAOM fraction could help equilibrate the

398 concurrent, though seemingly opposed, processes of SOM accrual and SOM mobilization in

399 soils. Fast-cycling MAOM fraction could briefly stabilize soluble C and N compounds during

400 periods when their concentrations are high, thereby acting as a temporary buffer against losses of

401 C and N via leaching, microbial respiration, and transformations like denitrification. For

402 example, in agroecosystems, the rapid, early season movement of inorganic N fertilizers into

403 microbial biomass and MAOM can enhance its availability later, during periods of peak crop

404 growth. When soluble SOM pools are low, desorption and decomposition of fast-cycling MAOM

405 could supply plants and microbes with energy and nutrients, and thus may regulate short-term

406 nutrient availability. Over time, some fast-cycling MAOM may form stronger bonds with

407 mineral surfaces or be incorporated into larger SOM complexes like aggregates, thereby

408 transforming it to slower-cycling MAOM. This pipeline of loss-prone dissolved compounds

409 moving through fast-cycling MAOM into persistent SOM may be key to increasing retention of

410 C, N, and other nutrients in the soil system.

411 Ultimately, the ecosystem and management implications of rapidly cycling MAOM

412 depend on the fate(s) of MAOM following desorption. Fast-cycling MAOM may be functionally

413 similar to POM, but the lower C:N ratio of MAOM suggests that it should be utilized relatively

414 efficiently by microbes, resulting in less CO_2 losses and greater C and N incorporation into

415 microbial biomass and metabolites compared to POM. This cycle of SOM temporarily sorbing to

416 mineral surfaces, undergoing microbial consumption and transformation, and re-release into soil

417 solution as DOM, has been suggested to result in the "cascade theory" of SOM downward

418 translocation[139]. This theory is supported by the observation of relatively older, more

419 microbially-processed SOM in deeper soil horizons, as well as by empirical observations of

420 DOM chemical composition changes during downward transport through grassland soil profiles

421 using ultrahigh-resolution mass spectrometry[140]. Specific surface soil management strategies

422 promoting SOC transport to, and accumulation within, deeper soils remain a critical knowledge

423 gap [141], and fast cycling MAOM may be key to this process. Research focusing specifically on

424 MAOM dynamics across soil depths could help clarify our understanding of the fate and

425 importance of fast-cycling MAOM in long-term C storage.

426

427 *5.2. Integrating fast-cycling MAOM into models of soil C and N dynamics*

428

429 Earth system models typically conceptualize soil carbon as multiple pools that decompose via

430 first-order decay kinetics and differ in their turnover times[142]. In the last decade, models that

431 explicitly include nonlinear microbial-mineral interactions are becoming more prevalent but vary

432 widely in their process representations and parameterizations [143–146]. Mechanisms of

433 stabilization vary from DOC sorption only [147,148] to accumulation of microbial necromass[146,149] or

434 chemically recalcitrant compounds [123] to a combination of the two [150–153]. As a result of these

435 different model formulations, the predicted temporal dynamics of SOM, and the underlying

436 pools conceptualized as MAOM, can vary widely in response to disturbance[143,154].

437 The vast majority of SOM models, including all models used at global scales, assume that

438 modeled pools are homogenous and that any particle within a pool has an equal probability of

439 entering or leaving as its neighbor[142]. Within this framework, turnover time and age is estimated

440 as a single value for each pool, such that representing MAOM of varying ages would require

441 increasing the number of pools and defining specific stabilization mechanisms or a combination

442 of mechanisms for each pool. However, when MAOM is explicitly represented in SOM models,

443 it is most often defined as a single pool[147,148,150,152]. Brunmayr et al. found that multiple of these

444 SOM models overestimate MAOM turnover and suggested further dividing the MAOM pool to

445 better represent components with different turnover times[155].

446 Select models do include a second MAOM pool that is considered faster cycling – for

447 example, the – for example, the 'exchangeable MAOM' pool in the MEMS v2 model[155], the 'Q'

448 pool in the MEND model [153], and the 'Q_DOM' pool in the COMISSION model[151], which all

449 represent DOC sorbed to minerals that can readily exchange with DOC in solution. However,

450 parameterizing sorption/desorption rates for these distinct MAOM pools, and benchmarking their

451 relative sizes, poses a significant challenge due to data limitations especially at larger scales.

452 Alternatively, other modeling frameworks exist that focus on a continuum of individual particles

453 traveling through model pools, with the ability to estimate the distribution of ages and transit

454   times within a single pool[53,156,157]. Models can also represent the fast-cycling MAOM pool by

455   allowing for MAOM desorption at relatively high rates; a study using the SOMic model, which

456   represents microbial dynamics and allows for rapid MAOM desorption, found that this modeling

457   framework generated predictions of global SOC distribution and long-term SOC dynamics that

458   were closely aligned with empirical data[158]. Regardless of the modeling framework, the existence

459   of fast-cycling MAOM suggests that modeling MAOM as a single homogenous, passively

460   cycling SOM pool is likely insufficient for accurately capturing temporal dynamics.

461

462   *5.3 Measurement of fast-cycling MAOM*

463

464   Although SOM fractionation methods drive our operational and conceptual understanding of

465   POM and MAOM pools, we lack a standard method for directly quantifying the fast-cycling

466   MAOM pool. MAOM can be further separated along physical (density, particle size) and

467   chemical (solubility in acid or base, oxidation, thermal lability) gradients, which may, in theory,

468   be able to isolate a more bioavailable subfraction. However, these methods also often require

469   further dispersion and disruption that may facilitate the inter-fraction transfer of C and N.

470   Common procedures for isolating SOM fractions may remove or obscure the fast-cycling portion

471   of MAOM. Fractionation procedures require a degree of mixing and dispersion in liquid that will

472   release and redistribute DOM between POM and MAOM. The quantity of DOM leached during

473   fractionation can be significant[159] and it is currently not possible to distinguish between POM or

474   MAOM in leached compounds. MAOM that desorbs and enters dissolved pools during

475   fractionation may be an important component of fast-cycling MAOM. More studies are needed

476   to identify the extent of leaching under contrasting fractionation and dispersion conditions as it is

477   possible that certain methods favor the transfer of POM C or N into the MAOM pool, potentially

478   inflating the stabilization capacity of this fraction.

479   Sequential chemical extractions can isolate phases of MAOM that differ in solubility and

480   potentially bioavailability. Selective dissolutions with Na-pyrophosphate, hydroxylamine, and

481   dithionite-HCl can be used to target organo-metal complexes, short-range order Al and Fe

482   hydroxides, and crystalline Fe hydroxides, respectively[160]. These well-stabilized forms of

483   MAOM are still vulnerable to loss, such as the iron-associated carbon that is destabilized and

484   released by low molecular weight organic acids or under saturated conditions[111,161]. Physical and

485   chemical fractionation methods can also be combined with thermal and/or chemometric

486   approaches to estimate the chemical and biological stability of particle size fractions of SOM[162].

487   Otherwise, a combined chemical and biological assay is a potentially promising method for

488   simulating destabilizing agents and the conditions that accelerate MAOM cycling. For example,

489   by incubating isolated MAOM fractions with organic acids and glucose to simulate root

490   exudates, one can estimate the destabilization potential of MAOM[163]. However, this has not been

491   examined comprehensively across soil types and experimental conditions to generate a standard

492   method.

493   Radiocarbon and ^{13}C-based experiments can provide estimates of pool turnover times.

494   However, these methods provide an average turnover time, which may obscure the smaller,

495   faster cycling subfraction, unless paired with ramped thermal analysis techniques that can

496   quantify an underlying distribution of turnover times. MAOM generally has a wide distribution

497   of radiocarbon mean ages, with considerable overlap with the distribution for POM [10,108].

498   Measurements of CO_2 respiration in long-term incubations can be used to calculate the size and

499   turnover rate of active and slow pools of C[164] although calculated residence times may vary

500 based on experiment duration[165] and these incubations are unable to determine the origin of the

501 CO_2. Isotope tracer-based experiments in which POM and MAOM fractions are differentially

502 labelled would allow for the tracing of fast-cycling MAOM and provide critical, mechanistic

503 insights into the potential size of and controls on this pool. In general, more research is needed to

504 identify a consistent method and guidance for how to pair fractionation methods with isotope

505 tracer and/or spectroscopic/imaging methods to isolate the various MAOM sub-fractions.

506

507

508 *6. Conclusion*

509

510 For decades, the soil science community has acknowledged the existence of fast-cycling

511 MAOM. Although the majority of MAOM is highly persistent and cycles on decadal and

512 millennial time-scales, a portion is bioavailable, exchangeable, and an active contributor to C and

513 N fluxes. As we have summarized, the size of this pool will likely depend on the intrinsic

514 properties of the MAOM – namely, the availability and physicochemical properties of minerals

515 as well as the composition, quantity, and structure of the associated organic matter. In addition,

516 fast-cycling MAOM will likely respond readily to drivers of destabilization, such as plant-

517 microbe interactions, climate change, agricultural intensification, and land use change.

518 Therefore, clarifying its size and responses in varying ecological scenarios is important to

519 improve model predictions and make better recommendations for land managers. While

520 counterintuitive to the goals of soil C sequestration, within certain contexts, it may be

521 desirable/beneficial to promote the existence of a fast-cycling MAOM pool. Accurate

522 quantification of this pool and its role in ecological processes will enhance our understanding of

523 these contexts and could inform agricultural management approaches. Likewise, our previous

524 understanding of MAOM as a persistent, slowly-aggrading pool is clearly oversimplified, and

525 including more realistic representations of fast-cycling MAOM in Earth system models is needed

526 to accurately quantify both the current and future size of this SOM pool. These applications are

527 currently hindered by methodological limitations that have made it challenging to characterize

528 this dynamic pool of MAOM. Continued development of methods to isolate and trace fast-

529 cycling MAOM will enable better quantification of this pool and subsequent integration of these

530 insights into modeling and soil management practices.

531

540

541 *8. Conflict of Interests Statement*
542 The authors declare no conflicts of interest.

543

544 **References**
545 1.   Grandy, A. S. & Neff, J. C. Molecular C dynamics downstream: The biochemical decomposition

546   sequence and its impact on soil organic matter structure and function. *Sci. Total Environ.* **404**, 297–

547   307 (2008).

548   2.   Heckman, K. *et al.* Beyond bulk: Density fractions explain heterogeneity in global soil carbon

549   abundance and persistence. *Glob. Change Biol.* **28**, 1178–1196 (2022).

550   3.   Torn, M. S., Trumbore, S. E., Chadwick, O. A., Vitousek, P. M. & Hendricks, D. M. Mineral

551   control of soil organic carbon storage and turnover. *Nature* **389**, 170–173 (1997).

552   4.   Lehmann, J., Kinyangi, J. & Solomon, D. Organic matter stabilization in soil microaggregates:

553   implications from spatial heterogeneity of organic carbon contents and carbon forms.

554   *Biogeochemistry* **85**, 45–57 (2007).

555   5.   Leuthold, S., Lavallee, J. M., Haddix, M. L. & Cotrufo, M. F. Contrasting properties of soil organic

556   matter fractions isolated by different physical separation methodologies. *Geoderma* **445**, 116870

557   (2024).

558   6.   Bu, R. *et al.* Particulate organic matter affects soil nitrogen mineralization under two crop rotation

559   systems. *PLoS ONE* **10**, (2015).

560   7.   Angst, G. *et al.* Unlocking complex soil systems as carbon sinks: multi-pool management as the

561   key. *Nat. Commun.* **14**, 2967 (2023).

562   8.   Chenu, C. & Plante, A. F. Clay-sized organo-mineral complexes in a cultivation chronosequence:

563   revisiting the concept of the 'primary organo-mineral complex'. *Eur. J. Soil Sci.* **57**, 596–607

564   (2006).

565   9.   Cotrufo, F. M. *et al.* Formation of soil organic matter via biochemical and physical pathways of

566   litter mass loss. *Nat. Geosci.* (2015) doi:10.1038/NGEO2520.

567   10. Cotrufo, M. F. & Lavallee, J. M. Chapter One - Soil organic matter formation, persistence, and

568   functioning: A synthesis of current understanding to inform its conservation and regeneration. in

569   *Advances in Agronomy* (ed. Sparks, D. L.) vol. 172 1–66 (Academic Press, 2022).

570   11. Totsche, K. U. *et al.* Microaggregates in soils. *J. Plant Nutr. Soil Sci.* **181**, 104–136 (2018).

571   12. Even, R. J. & Francesca Cotrufo, M. The ability of soils to aggregate, more than the state of

572   aggregation, promotes protected soil organic matter formation. *Geoderma* **442**, 116760 (2024).

573   13.   Sokol, N. W., Sanderman, J. & Bradford, M. A. Pathways of mineral-associated soil organic matter

574   formation: Integrating the role of plant carbon source, chemistry, and point of entry. *Glob. Change*

575   *Biol.* **25**, 12–24 (2019).

576   14.   Poirier, V. *et al.* Organo-Mineral Interactions Are More Important for Organic Matter Retention in

577   Subsoil Than Topsoil. *Soil Syst.* **4**, 4 (2020).

578   15.   Haddix, M. L., Paul, E. A. & Cotrufo, M. F. Dual, differential isotope labeling shows the

579   preferential movement of labile plant constituents into mineral-bonded soil organic matter. *Glob.*

580   *Change Biol.* **22**, 2301–2312 (2016).

581   16.   Fulton-Smith, S., Even, R. & Cotrufo, M. F. Depth impacts on the aggregate-mediated mechanisms

582   of root carbon stabilization in soil: Trade-off between MAOM and POM pathways. *Geoderma* **452**,

583   117078 (2024).

584   17.   Shabtai, I. A. *et al.* Calcium promotes persistent soil organic matter by altering microbial

585   transformation of plant litter. *Nat. Commun.* **14**, 6609 (2023).

586   18.   Angst, G. *et al.* Soil organic carbon stocks in topsoil and subsoil controlled by parent material,

587   carbon input in the rhizosphere, and microbial-derived compounds. *Soil Biol. Biochem.* **122**, 19–30

588   (2018).

589   19.   Barré, P., Fernandez-Ugalde, O., Virto, I., Velde, B. & Chenu, C. Impact of phyllosilicate

590   mineralogy on organic carbon stabilization in soils: incomplete knowledge and exciting prospects.

591   *Geoderma* **235–236**, 382–395 (2014).

592   20.   Bailey, V. L., Pries, C. H. & Lajtha, K. What do we know about soil carbon destabilization?

593   *Environ. Res. Lett.* **14**, 083004 (2019).

594   21.   Dynarski, K. A., Bossio, D. A. & Scow, K. M. Dynamic Stability of Soil Carbon: Reassessing the

595   "Permanence" of Soil Carbon Sequestration. *Front. Environ. Sci.* **8**, (2020).

596   22.   Piñeiro, G., Paruelo, J. M., Jobbágy, E., Jackson, R. B. & Oesterheld, M. Grazing effects on

597   belowground C and N stocks along a network of cattle exclosures in temperate and subtropical

598   grasslands of South America. *Glob. Biogeochem. Cycles* **23**, (2009).

599   23.   Woodmansee, R. G. & Duncan, D. A. Nitrogen and phosphorus dynamics and budgets in annual

600   grasslands. *Ecology* **61**, 893–904 (1980).

601   24.   Kleber, M., Sollins, P. & Sutton, R. A conceptual model of organo-mineral interactions in soils:

602   self-assembly of organic molecular fragments into zonal structures on mineral surfaces.

603   *Biogeochemistry* **85**, 9–24 (2007).

604   25.   Torn, M. S. *et al.* A dual isotope approach to isolate soil carbon pools of different turnover times.

605   *Biogeosciences* **10**, 8067–8081 (2013).

606   26.   Kleber, M. *et al.* Dynamic interactions at the mineral–organic matter interface. *Nat. Rev. Earth*

607   *Environ.* **2**, 402–421 (2021).

608   27.   Lavallee, J. M., Soong, J. L. & Cotrufo, M. F. Conceptualizing soil organic matter into particulate

609   and mineral-associated forms to address global change in the 21st century. *Glob. Change Biol.*

610   (2019) doi:10.1111/gcb.14859.

611   28.   Kleber, M. *et al.* Mineral-organic associations: formation, properties, and relevance in soil

612   environments. *Adv. Agron.* **130**, 1–140 (2015).

613   29.   Mikutta, R. *et al.* Biogeochemistry of mineral-organic associations across a long-term mineralogical

614   soil gradient (0.3-4100 kyr), Hawaiian Islands. *Geochim. Cosmochim. Acta* **73**, 2034–2060 (2009).

615   30.   Sanderman, J., Maddern, T. & Baldock, J. Similar composition but differential stability of mineral

616   retained organic matter across four classes of clay minerals. *Biogeochemistry* **121**, 409–424 (2014).

617   31.   Underwood, T. R., Bourg, I. C. & Rosso, K. M. Mineral-associated organic matter is heterogeneous

618   and structured by hydrophobic, charged, and polar interactions. *Proc. Natl. Acad. Sci.* **121**,

619   e2413216121 (2024).

620   32.   Kögel-Knabner, I. *et al.* Organo-mineral associations in temperate soils: Integrating biology,

621   mineralogy, and organic matter chemistry. *J. Plant Nutr. Soil Sci.* **171**, 61–82 (2008).

622   33.   Scheidegger, A. M. & Sparks, D. L. A critical assessment of sorption-desorption mechanisms at the

623   soil mineral/water interface. *Soil Sci.* **161**, 813 (1996).

624   34.   Bramble, D. S. E. *et al.* Formation of mineral-associated organic matter in temperate soils is

625   primarily controlled by mineral type and modified by land use and management intensity. *Glob.*

626   *Change Biol.* **30**, e17024 (2024).

627   35.   Deng, Y. & Dixon, J. B. Soil Organic Matter and Organic-Mineral Interactions. in *Soil Mineralogy*

628   *with Environmental Applications* 69–107 (John Wiley & Sons, Ltd, 2002).

629   doi:10.2136/sssabookser7.c3.

630   36.   Lv, J. *et al.* Molecular-Scale Investigation with ESI-FT-ICR-MS on Fractionation of Dissolved

631   Organic Matter Induced by Adsorption on Iron Oxyhydroxides. *Environ. Sci. Technol.* **50**, 2328–

632   2336 (2016).

633   37.   Oren, A. & Chefetz, B. Sorptive and Desorptive Fractionation of Dissolved Organic Matter by

634   Mineral Soil Matrices. *J. Environ. Qual.* **41**, 526–533 (2012).

635   38.   Kramer, M. C., Sanderman, J., Chadwick, O. A., Chorover, J. & Vitousek, P. M. Long - term carbon

636   storage through retention of dissolved aromatic acids by reactive particles in soil. *Glob. Change*

637   *Biol.* **18**, 2594–2605 (2012).

638   39.   Rocci, K. S. *et al.* Impacts of nutrient addition on soil carbon and nitrogen stoichiometry and

639   stability in globally-distributed grasslands. *Biogeochemistry* **159**, 353–370 (2022).

640   40.   Heckman, K. *et al.* Sorptive fractionation of organic matter and formation of organo-hydroxy-

641   aluminum complexes during litter biodegradation in the presence of gibbsite. *Geochim. Cosmochim.*

642   *Acta* **121**, 667–683 (2013).

643   41.   Inagaki, T. M. *et al.* Subsoil organo-mineral associations under contrasting climate conditions.

644   *Geochim. Cosmochim. Acta* **270**, 244–263 (2020).

645   42.   Keiluweit, M. *et al.* Nano-scale investigation of the association of microbial nitrogen residues with

646   iron (hydr)oxides in a forest soil O-horizon. *Geochim. Cosmochim. Acta* **95**, 213–226 (2012).

647   43.   Possinger, A. R. *et al.* Organo-mineral interactions and soil carbon mineralizability with variable

648   saturation cycle frequency. *Geoderma* **375**, 114483 (2020).

649   44.   Rillig, M. C., Caldwell, B. A., W??sten, H. A. B. & Sollins, P. Role of proteins in soil carbon and

650   nitrogen storage: Controls on persistence. *Biogeochemistry* **85**, 25–44 (2007).

651   45.   Spohn, M. Preferential adsorption of nitrogen- and phosphorus-containing organic compounds to

652   minerals in soils: A review. *Soil Biol. Biochem.* **194**, 109428 (2024).

653   46.   Kinyangi, J. *et al.* Nanoscale Biogeocomplexity of the Organomineral Assemblage in Soil. *Soil Sci.*

654   *Soc. Am. J.* **70**, 1708–1718 (2006).

655   47.   Lehmann, J. *et al.* Spatial complexity of soil organic matter forms at nanometre scales. *Nat. Geosci*

656   **1**, 238–242 (2008).

657   48.   Steffens, M. *et al.* Identification of Distinct Functional Microstructural Domains Controlling C

658   Storage in Soil. *Environ. Sci. Technol.* **51**, 12182–12189 (2017).

659   49.   Vogel, C. *et al.* Submicron structures provide preferential spots for carbon and nitrogen

660   sequestration in soils. *Nat. Commun.* **5**, 2947 (2014).

661   50.   Kaiser, K. & Guggenberger, G. Mineral surfaces and soil organic matter. *Eur J Soil Sci.* **54**, 219–

662   236 (2003).

663   51.   Kaiser, K. & Guggenberger, G. Sorptive stabilization of organic matter by microporous goethite:

664   sorption into small pores vs. surface complexation. *Eur. J. Soil Sci.* **58**, 45–59 (2007).

665   52.   Coward, E. K., Ohno, T. & Sparks, D. L. Direct Evidence for Temporal Molecular Fractionation of

666   Dissolved Organic Matter at the Iron Oxyhydroxide Interface. *Environ. Sci. Technol.* **53**, 642–650

667   (2019).

668   53.   Sierra, C. A., Hoyt, A. M., He, Y. & Trumbore, S. E. Soil Organic Matter Persistence as a

669   Stochastic Process: Age and Transit Time Distributions of Carbon in Soils. *Glob. Biogeochem.*

670   *Cycles* **32**, 1574–1588 (2018).

671   54.   Feng, W. *et al.* Methodological uncertainty in estimating carbon turnover times of soil fractions.

672   *Soil Biol. Biochem.* **100**, 118–124 (2016).

673   55.   Hall, S. J., McNicol, G., Natake, T. & Silver, W. L. Large fluxes and rapid turnover of mineral-

674   associated carbon across topographic gradients in a humid tropical forest: insights from paired 14C

675   analysis. *Biogeosciences* **12**, 2471–2487 (2015).

676   56.   Schrumpf, M. & Kaiser, K. Large differences in estimates of soil organic carbon turnover in density

677   fractions by using single and repeated radiocarbon inventories. *Geoderma* **239–240**, 168–178

678   (2015).

679   57.   Heckman, K. A. *et al.* Soil organic matter is principally root derived in an Ultisol under oak forest.

680   *Geoderma* **403**, 115385 (2021).

681   58.   Fox, P. M. *et al.* Shale as a Source of Organic Carbon in Floodplain Sediments of a Mountainous

682   Watershed. *J. Geophys. Res. Biogeosciences* **125**, e2019JG005419 (2020).

683   59.   Grant, K. E. *et al.* Diverse organic carbon dynamics captured by radiocarbon analysis of distinct

684   compound classes in a grassland soil. *Biogeosciences* **21**, 4395–4411 (2024).

685   60.   Schrumpf, M. *et al.* Storage and stability of organic carbon in soils as related to depth, occlusion

686   within aggregates, and attachment to minerals. *Biogeosciences* **10**, 1675–1691 (2013).

687   61.   Stoner, S. *et al.* Relating mineral–organic matter stabilization mechanisms to carbon quality and age

688   distributions using ramped thermal analysis. *Philos. Trans. R. Soc. Math. Phys. Eng. Sci.* **381**,

689   20230139 (2023).

690   62.   Allison, S. D. & Jastrow, J. D. Activities of extracellular enzymes in physically isolated fractions of

691   restored grassland soils. *Soil Biol. Biochem.* **38**, 3245–3256 (2006).

692   63.   Breulmann, M. *et al.* Short-term bioavailability of carbon in soil organic matter fractions of

693   different particle sizes and densities in grassland ecosystems. *Sci. Total Environ.* **497–498**, 29–37

694   (2014).

695   64.   Kandeler, E. *et al.* The mineralo-sphere – Succession and physiology of bacteria and fungi

696   colonising pristine minerals in grassland soils under different land-use intensities. *Soil Biol.*

697   *Biochem.* **136**, 107534 (2019).

698   65.   Jilling, A. *et al.* Minerals in the rhizosphere: overlooked mediators of soil nitrogen availability to

699   plants and microbes. *Biogeochemistry* (2018) doi:10.1007/s10533-018-0459-5.

700   66.   Yu, W., Huang, W., Weintraub-Leff, S. R. & Hall, S. J. Where and why do particulate organic

701   matter (POM) and mineral-associated organic matter (MAOM) differ among diverse soils? *Soil*

702   *Biol. Biochem.* **172**, 108756 (2022).

703   67.   Bailey, T. *et al.* Opposing patterns of carbon and nitrogen stability in soil organic matter fractions

704   compared to whole soil. *Eur. J. Soil Sci.* **75**, e13495 (2024).

705   68.   Bimüller, C. *et al.* Decoupled carbon and nitrogen mineralization in soil particle size fractions of a

706   forest topsoil. *Soil Biol. Biochem.* **78**, 263–273 (2014).

707   69.   Mueller, C. W. *et al.* Bioavailability and isotopic composition of CO2 released from incubated soil

708   organic matter fractions. *Soil Biol. Biochem.* **69**, 168–178 (2014).

709   70.   Parfitt, R. L. & Salt, G. J. Carbon and nitrogen mineralisation in sand, silt, and clay fractions of soils

710   under maize and pasture. *Aust. J. Soil Res. Aust J Soil Res* **39**, 361–371 (2001).

711   71.   Sollins, P., Spycher, G. & Glassman, C. A. Net nitrogen mineralization from light- and heavy-

712   fraction forest soil organic matter. *Soil Biol. Biochem.* **16**, 31–37 (1984).

713   72.   Whalen, J. K., Bottomley, P. J. & Myrold, D. D. Carbon and nitrogen mineralization from light- and

714   heavy-fraction additions to soil. *Soil Biol. Biochem.* **32**, 1345–1352 (2000).

715   73.   Villarino, S. H. *et al.* A large nitrogen supply from the stable mineral-associated soil organic matter

716   fraction. *Biol. Fertil. Soils* **59**, 833–841 (2023).

717   74.   Abramoff, R. Z. *et al.* How much carbon can be added to soil by sorption? *Biogeochemistry* **152**,

718   127–142 (2021).

719   75.   Neurath, R. A. *et al.* Root Carbon Interaction with Soil Minerals Is Dynamic, Leaving a Legacy of

720   Microbially Derived Residues. *Environ. Sci. Technol.* **55**, 13345–13355 (2021).

721   76.   Shabtai, I. A. *et al.* Root exudates simultaneously form and disrupt soil organo-mineral associations.

722   *Commun. Earth Environ.* **5**, 1–12 (2024).

723   77.   Chari, N. R. & Taylor, B. N. Soil organic matter formation and loss are mediated by root exudates
724   in a temperate forest. *Nat. Geosci.* **15**, 1011–1016 (2022).

725   78.   Kaštovská, E. *et al.* Root but not shoot litter fostered the formation of mineral-associated organic
726   matter in eroded arable soils. *Soil Tillage Res.* **235**, 105871 (2024).

727   79.   Sokol, N. W. *et al.* The path from root input to mineral-associated soil carbon is dictated by habitat-
728   specific microbial traits and soil moisture. *Soil Biol. Biochem.* **193**, 109367 (2024).

729   80.   Sokol, N. W. & Bradford, M. A. Microbial formation of stable soil carbon is more efficient from
730   belowground than aboveground input. *Nat. Geosci.* **12**, 46–53 (2019).

731   81.   Villarino, S. H., Pinto, P., Jackson, R. B. & Piñeiro, G. Plant rhizodeposition: A key factor for soil
732   organic matter formation in stable fractions. *Sci. Adv.* **7**, eabd3176 (2021).

733   82.   Bélanger, N., C^oté, B., Fyles, J. W., Courchesne, F. & Hendershot, W. H. Forest regrowth as the
734   controlling factor of soil nutrient availability 75 years after fire in a deciduous forest of Southern
735   Quebec. *Plant Soil* **262**, 363–272 (2004).

736   83.   Lovett, G. M. *et al.* Nutrient retention during ecosystem succession: a revised conceptual model.
737   *Front. Ecol. Environ.* **16**, 532–538 (2018).

738   84.   Phillips, R. P., Bernhardt, E. S. & Schlesinger, W. H. Elevated CO2 increases root exudation from
739   loblolly pine (Pinus taeda) seedlings as an N-mediated response. *Tree Physiol.* **29**, 1513–1523
740   (2009).

741   85.   Heckman, K. A. *et al.* Moisture-driven divergence in mineral-associated soil carbon persistence.
742   *Proc. Natl. Acad. Sci.* **120**, e2210044120 (2023).

743   86.   Seguin, V. *et al.* Mineral weathering in the rhizosphere of forested soils. in *Biogeochemistry of*
744   *Trace Elements in the Rhizpshere* 22–55 (2005).

745   87.   Hinsinger, P. & Jaillard, B. Root-induced release of interlayer potassium and vermiculitization of
746   phlogopite as related to potassium depletion in the rhizosphere of ryegrass. *J. Soil Sci.* **44**, 525–534
747   (1993).

748   88.   Uroz, S. *et al.* Bacterial weathering and its contribution to nutrient cycling in temperate forest

749   ecosystems. *Res. Microbiol.* **162**, 821–831 (2011).

750   89.   Zhang, Z., Huang, J., He, L. & Sheng, X. Distinct Weathering Ability and Populations of Culturable

751   Mineral-Weathering Bacteria in the Rhizosphere and Bulk Soils of Morus Alba. *Geomicrobiol. J.*

752   **33**, 39–45 (2016).

753   90.   Chabot, R., Antoun, H. & Cescas, M. P. Growth promotion of maize and lettuce by phosphate-

754   solubilizing Rhizobium leguminosarum biovar. phaseoli. *Plant Soil* **39**, 311–321 (1996).

755   91.   Vazquez, P., Holguin, G., Puente, M. E., Lopez-Cortes, a. & Bashan, Y. Phosphate-solubilizing

756   microorganisms associated with the rhizosphere of mangroves in a semiarid coastal lagoon. *Biol.*

757   *Fertil. Soils* **30**, 460–468 (2000).

758   92.   Calvaruso, C., Mareschal, L., Turpault, M.-P. & Leclerc, E. Rapid clay weathering in the

759   rhizosphere of norway spruce and oak in an acid forest ecosystem. *Soil Sci. Soc. Am. J.* **73**, 331

760   (2009).

761   93.   Mareschal, L., Turpault, M.-P., Bonnaud, P. & Ranger, J. Relationship between the weathering of

762   clay minerals and the nitrification rate: a rapid tree species effect. *Biogeochemistry* **112**, 293–309

763   (2013).

764   94.   Paola, A., Pierre, B., Vincenza, C., Vincenzo, D. M. & Bruce, V. Short term clay mineral release

765   and re-capture of potassium in a Zea mays field experiment. *Geoderma* **264**, 54–60 (2016).

766   95.   Tunlid, A., Floudas, D., Op De Beeck, M., Wang, T. & Persson, P. Decomposition of soil organic

767   matter by ectomycorrhizal fungi: Mechanisms and consequences for organic nitrogen uptake and

768   soil carbon stabilization. *Front. For. Glob. Change* **5**, (2022).

769   96.   Keiluweit, M. *et al.* Mineral protection of soil carbon counteracted by root exudates. *Nat. Clim.*

770   *Change* **5**, 588–595 (2015).

771   97.   Bonneville, S. *et al.* Tree-mycorrhiza symbiosis accelerate mineral weathering: Evidences from

772   nanometer-scale elemental fluxes at the hypha–mineral interface. *Geochim. Cosmochim. Acta* **75**,

773   6988–7005 (2011).

774   98.   Wang, T., Persson, P. & Tunlid, A. A widespread mechanism in ectomycorrhizal fungi to access

775   nitrogen from mineral-associated proteins. *Environ. Microbiol.* **23**, 5837–5849 (2021).

776   99.   Krumina, L., Op De Beeck, M., Meklesh, V., Tunlid, A. & Persson, P. Ectomycorrhizal Fungal

777   Transformation of Dissolved Organic Matter: Consequences for Reductive Iron Oxide Dissolution

778   and Fenton-Based Oxidation of Mineral-Associated Organic Matter. *Front. Earth Sci.* **10**, (2022).

779   100. Liu, F. *et al.* Production of reactive oxygen species and its role in mediating the abiotic

780   transformation of organic carbon in sandy soil under vegetation restoration. *Carbon Res.* **2**, 35

781   (2023).

782   101. Verbruggen, E., Struyf, E. & Vicca, S. Can arbuscular mycorrhizal fungi speed up carbon

783   sequestration by enhanced weathering? *PLANTS PEOPLE PLANET* **3**, 445–453 (2021).

784   102. Wu, S. *et al.* Soil organic matter dynamics mediated by arbuscular mycorrhizal fungi – an updated

785   conceptual framework. *New Phytol.* **242**, 1417–1425 (2024).

786   103. Fernandez, C. W., Langley, J. A., Chapman, S., McCormack, M. L. & Koide, R. T. The

787   decomposition of ectomycorrhizal fungal necromass. *Soil Biol. Biochem.* **93**, 38–49 (2016).

788   104. Andrino, A. *et al.* Production of Organic Acids by Arbuscular Mycorrhizal Fungi and Their

789   Contribution in the Mobilization of Phosphorus Bound to Iron Oxides. *Front. Plant Sci.* **12**, (2021).

790   105. King, A. E. *et al.* A soil matrix capacity index to predict mineral-associated but not particulate

791   organic carbon across a range of climate and soil pH. *Biogeochemistry* **165**, 1–14 (2023).

792   106. Kramer, M. G. & Chadwick, O. A. Climate-driven thresholds in reactive mineral retention of soil

793   carbon at the global scale. *Nat. Clim. Change* **8**, 1104–1108 (2018).

794   107. Possinger, A. R. *et al.* Climate Effects on Subsoil Carbon Loss Mediated by Soil Chemistry.

795   *Environ. Sci. Technol.* **55**, 16224–16235 (2021).

796   108. Rasmussen, C. *et al.* Beyond clay: towards an improved set of variables for predicting soil organic

797   matter content. *Biogeochemistry* **137**, 297–306 (2018).

798   109. Adhikari, D. *et al.* Dynamics of ferrihydrite-bound organic carbon during microbial Fe reduction.

799   *Geochim. Cosmochim. Acta* **212**, 221–233 (2017).

110. Huang, W. & Hall, S. J. Elevated moisture stimulates carbon loss from mineral soils by releasing protected organic matter. *Nat. Commun.* **8**, 1774 (2017).

111. Patzner, M. S. *et al.* Iron mineral dissolution releases iron and associated organic carbon during permafrost thaw. *Nat. Commun.* **11**, 6329 (2020).

112. Zhao, Q. *et al.* Coupled dynamics of iron and iron-bound organic carbon in forest soils during anaerobic reduction. *Chem. Geol.* **464**, 118–126 (2017).

113. Zhao, Q. *et al.* Oxidation of soil organic carbon during an anoxic-oxic transition. *Geoderma* **377**, 114584 (2020).

114. Lieberman, H. P., Rothman, M., von Sperber, C. & Kallenbach, C. M. Experimental flooding shifts carbon, nitrogen, and phosphorus pool distribution and microbial activity. *Biogeochemistry* **165**, 75–90 (2023).

115. Jilling, A., Sokol, N. W., Morán-Rivera, K. & Stuart Grandy, A. Wet-dry cycling influences the formation of mineral-associated organic matter and its sensitivity to simulated root exudates. *Geoderma* **445**, 116869 (2024).

116. von Lützow, M. & Kögel-Knabner, I. Temperature sensitivity of soil organic matter decomposition—what do we know? *Biol. Fertil. Soils* **46**, 1–15 (2009).

117. Georgiou, K. *et al.* Emergent temperature sensitivity of soil organic carbon driven by mineral associations. *Nat. Geosci.* **17**, 205–212 (2024).

118. Rocci, K. S., Lavallee, J. M., Stewart, C. E. & Cotrufo, M. F. Soil organic carbon response to global environmental change depends on its distribution between mineral-associated and particulate organic matter: A meta-analysis. *Sci. Total Environ.* **793**, 148569 (2021).

119. He, N., Chen, Q., Han, X., Yu, G. & Li, L. Warming and increased precipitation individually influence soil carbon sequestration of Inner Mongolian grasslands, China. *Agric. Ecosyst. Environ.* **158**, 184–191 (2012).

824   120. Phillips, C. L., Murphey, V., Lajtha, K. & Gregg, J. W. Asymmetric and symmetric warming

825   increases turnover of litter and unprotected soil C in grassland mesocosms. *Biogeochemistry* **128**,

826   217–231 (2016).

827   121. Luo, Y. *et al.* Progressive Nitrogen Limitation of Ecosystem Responses to Rising Atmospheric

828   Carbon Dioxide. *BioScience* **54**, 731–739 (2004).

829   122. Rocci, K. S. *et al.* Bridging 20 Years of Soil Organic Matter Frameworks: Empirical Support,

830   Model Representation, and Next Steps. *J. Geophys. Res. Biogeosciences* **129**, e2023JG007964

831   (2024).

832   123. Sulman, B. N., Phillips, R. P., Oishi, a. C., Shevliakova, E. & Pacala, S. W. Microbe-driven

833   turnover offsets mineral-mediated storage of soil carbon under elevated CO2. *Nat. Clim. Change* **4**,

834   1099–1102 (2014).

835   124. Cotrufo, M. F., Wallenstein, M. D., Boot, C. M., Denef, K. & Paul, E. The Microbial Efficiency-

836   Matrix Stabilization (MEMS) framework integrates plant litter decomposition with soil organic

837   matter stabilization: do labile plant inputs form stable soil organic matter? *Glob. Change Biol.* **19**,

838   988–995 (2013).

839   125. Cates, A. M., Jilling, A., Tfaily, M. M. & Jackson, R. D. Temperature and moisture alter organic

840   matter composition across soil fractions. *Geoderma* **409**, 115628 (2022).

841   126. Leitner, Z. R., Daigh, A. L. M. & DeJong-Hughes, J. Temporal fluctuations of microbial

842   communities within the crop growing season. *Geoderma* **391**, 114951 (2021).

843   127. Fu, Z., Hu, W., Beare, M. & Baird, D. Soil macroaggregate-occluded mineral-associated organic

844   carbon drives the response of soil organic carbon to land use change. *Soil Tillage Res.* **244**, 106271

845   (2024).

846   128. Connell, R. K., James, T. Y. & Blesh, J. A legume-grass cover crop builds mineral-associated

847   organic matter across variable agricultural soils. *Soil Biol. Biochem.* **203**, 109726 (2025).

848   129. Mayer, M. *et al.* Dynamic stability of mineral-associated organic matter: enhanced stability and

849   turnover through organic fertilization in a temperate agricultural topsoil. *Soil Biol. Biochem.* **184**,

850   109095 (2023).

851   130. Daly, A. B. *et al.* A holistic framework integrating plant-microbe-mineral regulation of soil

852   bioavailable nitrogen. *Biogeochemistry* **154**, 211–229 (2021).

853   131. Rui, Y. *et al.* Persistent soil carbon enhanced in Mollisols by well-managed grasslands but not

854   annual grain or dairy forage cropping systems. *Proc. Natl. Acad. Sci.* **119**, e2118931119 (2022).

855   132. Kauer, K., Pärnpuu, S., Talgre, L., Eremeev, V. & Luik, A. Soil Particulate and Mineral-Associated

856   Organic Matter Increases in Organic Farming under Cover Cropping and Manure Addition.

857   *Agriculture* **11**, 903 (2021).

858   133. van der Pol, L. K. *et al.* Addressing the soil carbon dilemma: Legumes in intensified rotations

859   regenerate soil carbon while maintaining yields in semi-arid dryland wheat farms. *Agric. Ecosyst.*

860   *Environ.* **330**, 107906 (2022).

861   134. Osterholz, W. R. *et al.* Predicting Gross Nitrogen Mineralization and Potentially Mineralizable

862   Nitrogen using Soil Organic Matter Properties. *Soil Sci. Soc. Am. J.* **81**, 1115–1126 (2017).

863   135. Spackman, J. A., Fernández, F. G., Paiao, G. D., Venterea, R. T. & Coulter, J. A. Corn 15N uptake

864   and partitioning in response to fertilizer application rate and timing. *Agron. J.* **116**, 1991–2006

865   (2024).

866   136. White, C. M., Finney, D. M., Kemanian, A. R. & Kaye, J. P. Modeling the contributions of nitrogen

867   mineralization to yield of corn. *Agron. J.* **113**, 490–503 (2021).

868   137. Zhang, Z., Kaye, J. P., Bradley, B. A., Amsili, J. P. & Suseela, V. Cover crop functional types

869   differentially alter the content and composition of soil organic carbon in particulate and mineral-

870   associated fractions. *Glob. Change Biol.* **28**, 5831–5848 (2022).

871   138. Teixeira, R. da S. *et al.* Land-use change with pasture and short rotation eucalypts impacts the soil C

872   emissions and organic C stocks in the Cerrado biome. *Land Degrad. Dev.* **31**, 909–923 (2020).

873 139. Kaiser, K. & Kalbitz, K. Cycling downwards – dissolved organic matter in soils. *Soil Biol. Biochem.*

874   **52**, 29–32 (2012).

875 140. Roth, V.-N. *et al.* Persistence of dissolved organic matter explained by molecular changes during its

876   passage through soil. *Nat. Geosci.* **12**, 755–761 (2019).

877 141. Cagnarini, C. *et al.* Zones of influence for soil organic matter dynamics: A conceptual framework

878   for data and models. *Glob. Change Biol.* **25**, 3996–4007 (2019).

879 142. Todd-Brown, K. E. O. *et al.* Causes of variation in soil carbon simulations from CMIP5 Earth

880   system models and comparison with observations. *Biogeosciences* **10**, 1717–1736 (2013).

881 143. Sulman, B. N. *et al.* Multiple models and experiments underscore large uncertainty in soil carbon

882   dynamics. *Biogeochemistry* **141**, 109–123 (2018).

883 144. Todd-Brown, K. E. O., Hopkins, F. M., Kivlin, S. N., Talbot, J. M. & Allison, S. D. A framework

884   for representing microbial decomposition in coupled climate models. *Biogeochemistry* **109**, 19–33

885   (2012).

886 145. Treseder, K. K. *et al.* Integrating microbial ecology into ecosystem models: challenges and

887   priorities. *Biogeochemistry* **109**, 7–18 (2012).

888 146. Wieder, W. R., Grandy, A. S., Kallenbach, C. M. & Bonan, G. B. Integrating microbial physiology

889   and physio-chemical principles in soils with the MIcrobial-MIneral Carbon Stabilization (MIMICS)

890   model. *Biogeosciences* **11**, 3899–3917 (2014).

891 147. Ahrens, B., Braakhekke, M. C., Guggenberger, G., Schrumpf, M. & Reichstein, M. Contribution of

892   sorption, DOC transport and microbial interactions to the 14C age of a soil organic carbon profile:

893   Insights from a calibrated process model. *Soil Biol. Biochem.* **88**, 390–402 (2015).

894 148. Tang, J. & Riley, W. J. Weaker soil carbon–climate feedbacks resulting from microbial and abiotic

895   interactions. *Nat. Clim. Change* **5**, 56–60 (2015).

896 149. Wieder, W. R., Grandy, A. S., Kallenbach, C. M., Taylor, P. G. & Bonan, G. B. Representing life in

897   the Earth system with soil microbial functional traits in the MIMICS model. *Geosci. Model Dev.* **8**,

898   1789–1808 (2015).

899   150.   Abramoff, R. *et al.* The Millennial model: in search of measurable pools and transformations for

900   modeling soil carbon in the new century. *Biogeochemistry* **137**, 51–71 (2018).

901   151.   Ahrens, B. *et al.* Combination of energy limitation and sorption capacity explains 14C depth

902   gradients. *Soil Biol. Biochem.* **148**, 107912 (2020).

903   152.   Robertson, A. D. *et al.* Unifying soil organic matter formation and persistence frameworks: the

904   MEMS model. *Biogeosciences* **16**, 1225–1248 (2019).

905   153.   Wang, G., Post, W. M. & Mayes, M. A. Development of microbial-enzyme-mediated

906   decomposition model parameters through steady-state and dynamic analyses. *Ecol. Appl.* **23**, 255–

907   272 (2013).

908   154.   Wieder, W. R. *et al.* Simulating Global Terrestrial Carbon and Nitrogen Biogeochemical Cycles

909   With Implicit and Explicit Representations of Soil Microbial Activity. *J. Adv. Model. Earth Syst.*

910   **16**, e2023MS004156 (2024).

911   155.   Zhang, Y. *et al.* Simulating measurable ecosystem carbon and nitrogen dynamics with the

912   mechanistically defined MEMS 2.0 model. *Biogeosciences* **18**, 3147–3171 (2021).

913   156.   Agren, G. I. & Bosatta, N. Theoretical Analysis of the Long-Term Dynamics of Carbon and

914   Nitrogen in Soils. *Ecology* **68**, 1181–1189 (1987).

915   157.   Waring, B. G. *et al.* From pools to flow: The PROMISE framework for new insights on soil carbon

916   cycling in a changing world. *Glob. Change Biol.* (2020) doi:10.1111/gcb.15365.

917   158.   Woolf, D. & Lehmann, J. Microbial models with minimal mineral protection can explain long-term

918   soil organic carbon persistence. *Sci. Rep.* **9**, 6522 (2019).

919   159.   Plaza, C., Giannetta, B., Benavente, I., Vischetti, C. & Zaccone, C. Density-based fractionation of

920   soil organic matter: effects of heavy liquid and heavy fraction washing. *Sci. Rep.* **9**, 10146 (2019).

921   160.   Heckman, K., Lawrence, C. R. & Harden, J. W. A sequential selective dissolution method to

922   quantify storage and stability of organic carbon associated with Al and Fe hydroxide phases.

923   *Geoderma* **312**, 24–35 (2018).

924   161. Li, H. *et al.* Simple Plant and Microbial Exudates Destabilize Mineral-Associated Organic Matter

925   via Multiple Pathways. *Environ. Sci. Technol.* **55**, 3389–3398 (2021).

926   162. Schiedung, M., Barré, P. & Peoplau, C. Separating fast from slow cycling soil organic carbon – A

927   multi-method comparison on land use change sites. *Geoderma* **453**, 117154 (2025).

928   163. Jilling, A., Keiluweit, M., Gutknecht, J. L. M. & Grandy, A. S. Priming mechanisms providing

929   plants and microbes access to mineral-associated organic matter. *Soil Biol. Biochem.* **158**, 108265

930   (2021).

931   164. Paul, E. A., Morris, S. J. & Böhm, S. The determination of soil C pool sizes and turnover rates:

932   biophysical fractionation and tracers. in *Assessment Methods for Soil Carbon* 193–206 (CRC Press,

933   2000).

934   165. Paul, E. A., Morris, S. J., Conant, R. & Plante, A. F. Does the Acid Hydrolysis–Incubation Method

935   Measure Meaningful Soil Organic Carbon Pools? *Soil Sci. Soc. Am. J.* **70**, 1023–1035 (2006).

936   166. Konrad, A. *et al.* Microbial carbon use efficiency of mineral-associated organic matter is related to

937   its desorbability. *Soil Biol. Biochem.* **203**, 109740 (2025).

938   167. Jagadamma, S., Steinweg, J. M., Mayes, M., Wang, G. & Post, W. Decomposition of added and

939   native organic carbon from physically separated fractions of diverse soils. *Biol. Fertil. Soils* 1–9

940   (2013) doi:10.1007/s00374-013-0879-2.

941   168. Jones, D. L. & Edwards, A. C. Influence of sorption on the biological utilization of two simple

942   carbon substrates. *Soil Biol. Biochem.* **30**, 1895–1902 (1998).

943   169. McGhee, I., Sannino, F., Gianfreda, L. & Burns, R. G. Bioavailability of 2,4-D sorbed to a chlorite-

944   like complex. *Chemosphere* **39**, 285–291 (1999).

945   170. Mikutta, R. *et al.* Biodegradation of forest floor organic matter bound to minerals via different

946   binding mechanisms. *Geochim. Cosmochim. Acta* **71**, 2569–2590 (2007).

947   171. Saidy, A. R., Smernik, R. J., Baldock, J. A., Kaiser, K. & Sanderman, J. Microbial degradation of

948   organic carbon sorbed to phyllosilicate clays with and without hydrous iron oxide coating. *Eur. J.*

949   *Soil Sci.* **66**, 83–94 (2015).

950   172. Singh, N. *et al.* Bioavailability of an Organophosphorus Pesticide, Fenamiphos, Sorbed on an

951   Organo Clay. *J. Agric. Food Chem.* **51**, 2653–2658 (2003).

952   173. Gu, B., Schmitt, J., Chen, Z., Llang, L. & Mccarthyt, J. F. Adsorption and Desorption of Natural

953   Organic Matter on Iron Oxide: Mechanisms and Models. *Env. Sci Technol* **28**, 38–48 (1994).

954   174. Gu, B., Schmitt, J., Chen, Z., Liang, L. & McCarthy, J. F. Adsorption and desorption of different

955   organic matter fractions on iron oxide. *Geochim. Cosmochim. Acta* **59**, 219–229 (1995).

956   175. Joo, J. C., Shackelford, C. D. & Reardon, K. F. Association of humic acid with metal (hydr)oxide-

957   coated sands at solid–water interfaces. *J. Colloid Interface Sci.* **317**, 424–433 (2008).

958   176. Kahle, M., Kleber, M. & Jahn, R. Retention of dissolved organic matter by phyllosilicate and soil

959   clay fractions in relation to mineral properties. *Org. Geochem.* **35**, 269–276 (2004).

960   177. Kaiser, K. & Zech, W. Release of Natural Organic Matter Sorbed to Oxides and a Subsoil. *Soil Sci.*

961   *Soc. Am. J.* **63**, 1157–1166 (1999).

962   178. Konrad, A. *et al.* Microbial carbon use efficiency of mineral-associated organic matter is related to

963   its desorbability. *Soil Biol. Biochem.* **203**, 109740 (2025).

964   179. Navon, R., Hernandez-Ruiz, S., Chorover, J. & Chefetz, B. Interactions of Carbamazepine in Soil:

965   Effects of Dissolved Organic Matter. *J. Environ. Qual.* **40**, 942–948 (2011).

966   180. Saidy, A. R., Smernik, R. J., Baldock, J. A., Kaiser, K. & Sanderman, J. The sorption of organic

967   carbon onto differing clay minerals in the presence and absence of hydrous iron oxide. *Geoderma*

968   **209–210**, 15–21 (2013).

969   181. Singh, M., Sarkar, B., Biswas, B., Churchman, J. & Bolan, N. S. Adsorption-desorption behavior of

970   dissolved organic carbon by soil clay fractions of varying mineralogy. *Geoderma* **280**, 47–56

971   (2016).

972   182. Singh, M. *et al.* Influence of physico-chemical properties of soil clay fractions on the retention of

973   dissolved organic carbon. *Environ. Geochem. Health* **39**, 1335–1350 (2017).

974   183. Yeasmin, S. *et al.* Influence of mineral characteristics on the retention of low molecular weight

975   organic compounds: A batch sorption-desorption and ATR-FTIR study. *J. Colloid Interface Sci.*

976   **432**, 246–257 (2014).

977
978

979   **Figure Captions**

980

981   Figure 1. Conceptual figure illustrating the controls on MAOM chemical heterogeneity and three

982   known drivers of MAOM destabilization

983

984

985

986

987 Table 1. Results of mineralization experiments that provide evidence for the fast-cycling MAOM pool. Such studies measure respiration of

988 isotope-labeled compounds adsorbed to a pure clay or MAOM fraction. The method used in each paper is described alongside the clay or soil type

989 studied or employed in each experiment, and the primary results of said experiment.

Reference	Method	Clay or soil type	Substrate mineralization / bioavailability
166	^{14}C-labeled organic monomers (e.g., citric acid) adsorbed to pure minerals, mixed with soil, and incubated for three weeks; ^{14}C traced into microbial biomass. ^{14}C-CO_2 evolution was monitored during the first three weeks and for an additional three weeks after priming with glucose.	Kaolinite, illite, and goethite in loamy vs sandy arable topsoils	Substrate mineralization up to > 80% (citric acid on kaolinite and illite) and incorporation into microbial biomass up to ~65% (acetylglucosamine on kaolinite) over three weeks of incubation; subsequent glucose-induced priming, especially of organic acids, was highest in goethite
167	Particulate (POM) and mineral-associated (MAOM) fractions incubated with unlabeled or ^{14}C-labelled glucose for 150 days to measure total C and ^{14}C respiration.	Soils from five orders (Mollisol, Ultisol, Oxisol, Andisol, Gelisol) over four climate zones (temperate, tropics, sub-arctic, and arctic)	62–70% of glucose added to MAOM and 3–11% of native C from MAOM were respired over 150 days.
168	^{14}C-labeled citrate or glucose were equilibrated with minerals then incubated for 24 h in oxygenated suspension with or without bacteria cultured from grassland soil to quantify ^{14}C recovery in respired CO_2, in the solid phase (bacteria and minerals), and in supernatant	Synthetic illite-mica; pure kaolinite; synthetic ferric hydroxide (ferrihydrite); and a mixed clay subsoil containing kaolinite, illite/smectite, and goethite	40-60% of glucose C in all mineral treatments and 65% of citrate C sorbed to illite-mica were microbially respired within 6 h, but only 25%, 12%, and 1% of citrate C were respectively respired from kaolinite, mixed subsoil clay, and ferric hydroxide treatments
169	A ^{14}C-labeled organic compound (herbicide 2,4-D [dichloro-phenoxyacetic acid]) was sorbed to a mineral complex and incubated with cultured *Pseudomonas* sp.; ^{14}C in respired CO_2, solid, and liquid fractions measured after 28 days	An Al(OH)x-montmorillonite (chlorite-like) complex	Over 28 days, the bacteria desorbed or mineralized 80% of the sorbed 2,4-D, compared to 45% released by abiotic desorption alone

Reference	Method	Clay or soil type	Substrate mineralization / bioavailability
170	Organic matter (OM) extracted from forest floor O-horizon was sorbed onto minerals in the presence of different electrolytes to model the relative contributions of Ca^{2+} bridging and ligand exchange to organo-mineral binding mechanisms in solution, and aerobically incubated with O-horizon microbial inocula for 90 d to measure substrate respiration as CO2	Synthetic goethite (iron oxide); and purchased pyrophyllite and vermiculite	24-77% of OM was bioavailable after sorption to the minerals tested, and OM mineralization increased by 42-62%. Ca^{2+} bridging slightly increased OM bioavailability in goethite, but decreased OM bioavailability by 40-55% in pyrophylite and vermiculite; ligand exchange reduced OM bioavailability by 12%, 46%, and 66% respectively in vermiculite, pyrophylite, and goethite
171	Dissolved organic carbon (DOC) from plant residue loaded onto minerals was inoculated with soil extracts and incubated for 120 d to assess OC mineralization as CO_2	Kaolinite, illite, and smectite, with and without coatings of goethite, hematite, and ferrihydrite	13–24% of sorbed OC was mineralized over 120 days; mineral associations reduced OC bioavailability by 27-43%
172	An organo-clay complex of fenamiphos, an organophosphorus pesticide, was incubated in aqueous suspension in abiotic conditions or with added *Brevibacterium* sp., and pesticide desorption and hydrolysis was monitored by HPLC over 24 h	Cetyltrimethylammonium (CTMA)-exchanged montmorillonite clay	Bacteria hydrolyzed fenamiphos at a rate 77% greater than the abiotic desorption rate over 24 h, indicating high bioavailability despite strong interlayer sorption; 82% of the pesticide was hydrolyzed in inoculated samples versus 3% and 4.6% respectively degraded and desorbed in abiotic controls. Added enzymes penetrated the mineral interlayer and retained hydrolytic activity even when sorbed

990
991
992
993
994

Table 2. Results of batch (ad)sorption-desorption experiments that highlight the wide-ranging rate of OM desorption from minerals. The mineral type employed in each study is presented alongside the organic compounds that were sorbed/desorbed to said minerals, the experimental conditions, and the primary results of each study. For studies that report a hysteresis coefficient: this metric refers to the ratio of the slope of the sorption curve to the slope of the desorption curve. It is a measure of adsorption-desorption reversibility where an h of 0 indicates completely reversible and an h of 1 indicates completely irreversible.

Reference	Mineral type	Organic compounds	Experimental conditions	Results
173	Commercial iron oxide powder	Natural organic matter (NOM), collected from wetland pond	Acid (HCl), base (NaOH), or inorganic salts (NaCl, Na_2SO_4, Na_3PO_4) added before adsorption	Hysteresis coefficient (h) between 0.72 and 0.86 for pH 4.1 and between 0.78 and 0.92 for pH 6.0, indicating that desorption was very limited
174	Iron oxide powder	NOM from wetland pond, separated into hydrophobic and hydrophilic fractions	Acid (HCl), base (NaOH), or inorganic salts (NaCl, Na_2SO_4, Na_3PO_4) added before adsorption	Hysteresis coefficient (h) between 0.81 and 0.91 for hydrophobic NOM, h between 0.821 and 0.984 for hydrophilic NOM, indicating desorption was very limited
175	Uncoated, FeO(OH)-coated, and Al_2O_3-coated sands	Terrestrial humic acid extracted from commercially available peat	Uncoated vs (hydr)oxide coated sands	At pH 4.1, hysteresis coefficient (h) between 0.70 and 0.96 for metal (hydr)oxide coated sands, indicating limited desorption. For uncoated sands, h was between 0.41 and 0.78, suggesting higher desorption potential
176	Soils (Vitric Phaeozem, Haplic Chernozem, Chromic Luvisol, Calcaric Phaeozem, and Chromic Cambisol) and phyllosilicate clay fractions (Ca-montmorillonite, kaolinite, and illite)	Dissolved organic carbon (DOC) extracted from pine forest floor	Near-neutral pH; phosphate treatment used to block reactive hydroxyl groups	In samples without phosphate treatment, between 13% and 50% of DOC was desorbed, with greater desorption in the phyllosilicate clay compared to the soil clay fractions
177	Amorphous $Al(OH)_3$, goethite, and low organic C subsoil	NOM, extracted from Oa horizon of an Entic Haplorthod	Desorption using solutions with a range of pH and inorganic anions (Cl^-, SO_4^{2-}, and $H_2PO_4^-$)	Under normal conditions, desorption of NOM was <3%, desorption reached 60% in the presence of high concentrations of $H_2PO_4^-$
178	Kaolinite, illite, and geothite	14C-labelled monomers (glucose, acetylglucosamine,	Also measured microbial carbon use efficiency (CUE)	40-99% of monomers across all treatments were retained after desorption with NaN_3, the

Reference	Mineral type	Organic compounds	Experimental conditions	Results
		phenylalanine, salicylic acid, and citric acid)		range was reduced to 3-55% after subsequent desorption using PO_4^{3-}
179	Vertisol soil from crop field (bulk soil and its clay size fraction)	Carbamazepine (CBZ)	No CBZ, CBZ co-introduced, or CBZ introduced after DOM pre-adsorption	The hysteresis coefficient (HI) for CBZ-clay was 0.91 versus 0.64 in CBZ-bulk soil, HI decreased following pre-adsorption of DOM
37	Organic matter-poor, alkaline soils (Fluvent, Rhodoxeralf, and Loess)	DOM extracted from mature composted biosolids	Four sequential desorption steps	Up to 83% of sorbed DOM was retained after desorption
180	Pure clays (kaolinite, illite, smectite) with and without Fe oxide (haematite, goethite, ferrihydrite) coatings	DOC extracted from medic shoot	Effect of goethite coating on different clay types, effects of different Fe oxide coatings on illite	Across all treatments, 5.7–14.4% of sorbed DOC was desorbed
181	Soil clay fractions (kaolinite-illite, smectite, and allophane)	DOC extracted from wheat straw	Adsorption measured under varying electrolyte conditions: 0.1M and 0.01M $Ca(NO_3)_2$ and $NaNO_3$	6.4% to 55.3% of adsorbed DOC was desorbed
182	Soil clay fractions (kaolinite–illite, smectite, allophane)	DOC extracted from wheat straw	Untreated clay, C removed, and sesquioxide removed	30% to 71% of adsorbed DOC was desorbed across clay type; highest desorption in kaolinite-illite
183	Pure minerals (kaolinite, illite, montmorillonite, ferrihydrite, and goethite)	14C-labelled carboxylic acids and amino acids		For carboxylic acids: Fe oxides retained 83–100%, while phyllosilicates retained 31–85%. For amino acids: glutamic acid retention was 53–98% on Fe oxides versus 0–48% on phyllosilicates; lysine retention was 41–99% on phyllosilicates and 13–50% on Fe oxides
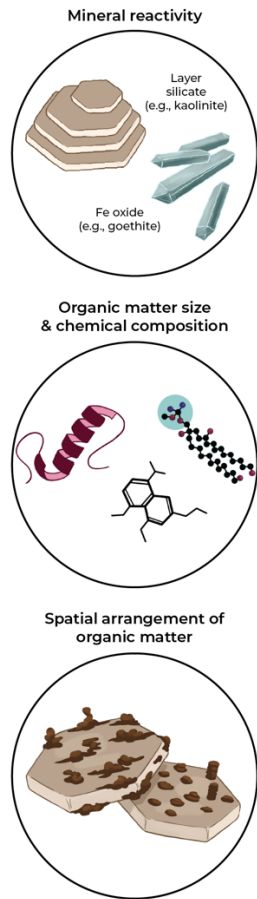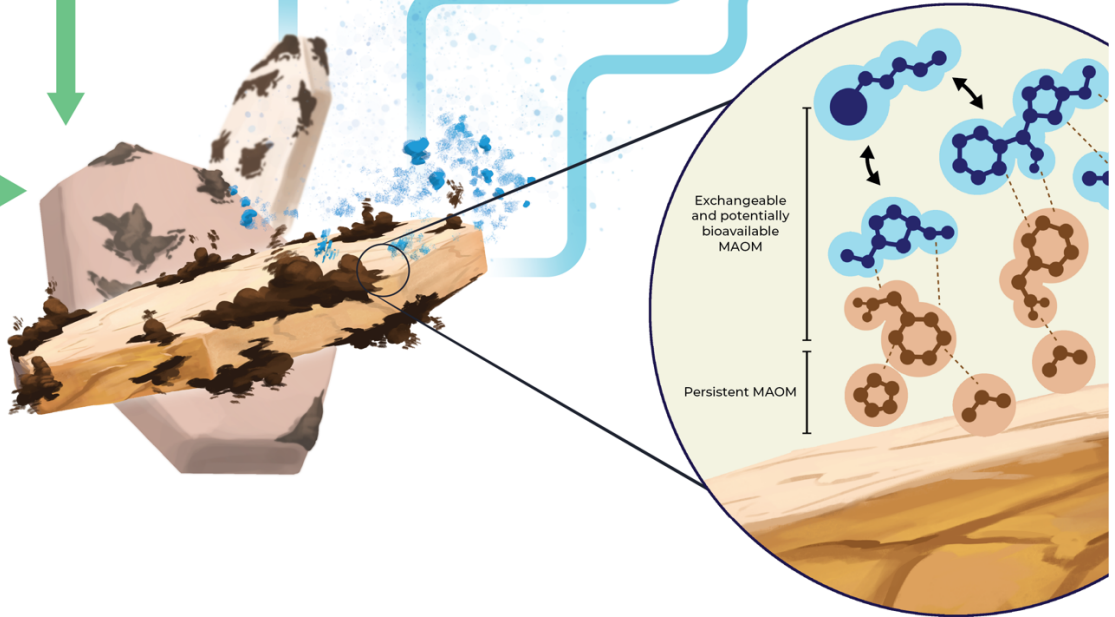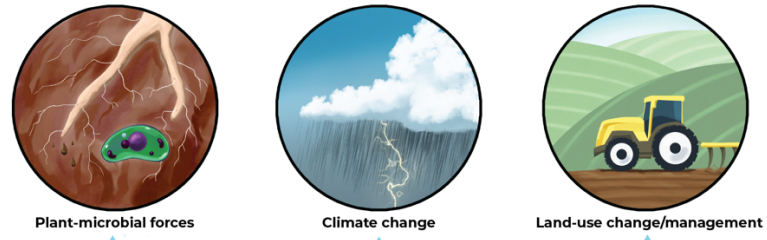
1000

1001   Figure 1. Conceptual figure illustrating the controls on MAOM chemical heterogeneity and three known drivers of MAOM

1002   destabilization

5